

UC Davis

UC Davis Previously Published Works

Title

Collision energy dependence of moments of net-kaon multiplicity distributions at RHIC

Permalink

<https://escholarship.org/uc/item/2z34081k>

Authors

Adamczyk, L
Adams, JR
Adkins, JK
et al.

Publication Date

2018-10-01

DOI

10.1016/j.physletb.2018.07.066

Peer reviewed

Collision Energy Dependence of Moments of Net-Kaon Multiplicity Distributions at RHIC

L. Adamczyk,¹ J. R. Adams,²⁹ J. K. Adkins,¹⁹ G. Agakishiev,¹⁷ M. M. Aggarwal,³¹ Z. Ahammed,⁵¹
 N. N. Ajitanand,⁴⁰ I. Alekseev,^{15, 26} D. M. Anderson,⁴² R. Aoyama,⁴⁶ A. Aparin,¹⁷ D. Arkhipkin,³
 E. C. Aschenauer,³ M. U. Ashraf,⁴⁵ A. Attri,³¹ G. S. Averichev,¹⁷ X. Bai,⁷ V. Bairathi,²⁷ K. Barish,⁴⁸ A. Behera,⁴⁰
 R. Bellwied,⁴⁴ A. Bhasin,¹⁶ A. K. Bhati,³¹ P. Bhattarai,⁴³ J. Bielcik,¹⁰ J. Bielcikova,¹¹ L. C. Bland,³
 I. G. Bordyuzhin,¹⁵ J. Bouchet,¹⁸ J. D. Brandenburg,³⁶ A. V. Brandin,²⁶ D. Brown,²³ I. Bunzarov,¹⁷
 J. Butterworth,³⁶ H. Caines,⁵⁵ M. Calderón de la Barca Sánchez,⁵ J. M. Campbell,²⁹ D. Cebrá,⁵ I. Chakaberia,³
 P. Chaloupka,¹⁰ Z. Chang,⁴² N. Chankova-Bunzarova,¹⁷ A. Chatterjee,⁵¹ S. Chattopadhyay,⁵¹ J. H. Chen,³⁹
 X. Chen,²¹ X. Chen,³⁷ J. Cheng,⁴⁵ M. Cherney,⁹ W. Christie,³ G. Contin,²² H. J. Crawford,⁴ S. Das,⁷
 L. C. De Silva,⁹ R. R. Debbe,³ T. G. Dedovich,¹⁷ J. Deng,³⁸ A. A. Derevschikov,³³ L. Didenko,³ C. Dilks,³²
 X. Dong,²² J. L. Drachenberg,²⁰ J. E. Draper,⁵ L. E. Dunkelberger,⁶ J. C. Dunlop,³ L. G. Efimov,¹⁷ N. Elsey,⁵³
 J. Engelage,⁴ G. Eppley,³⁶ R. Esha,⁶ S. Esumi,⁴⁶ O. Evdokimov,⁸ J. Ewigleben,²³ O. Eysen,³ R. Fatemi,¹⁹
 S. Fazio,³ P. Federic,¹¹ P. Federicova,¹⁰ J. Fedorisin,¹⁷ Z. Feng,⁷ P. Filip,¹⁷ E. Finch,⁴⁷ Y. Fisyak,³ C. E. Flores,⁵
 J. Fujita,⁹ L. Fulek,¹ C. A. Gagliardi,⁴² D. Garand,³⁴ F. Geurts,³⁶ A. Gibson,⁵⁰ M. Girard,⁵² D. Grosnick,⁵⁰
 D. S. Gunarathne,⁴¹ Y. Guo,¹⁸ S. Gupta,¹⁶ A. Gupta,¹⁶ W. Guryn,³ A. I. Hamad,¹⁸ A. Hamed,⁴² A. Harlenderova,¹⁰
 J. W. Harris,⁵⁵ L. He,³⁴ S. Heppelmann,⁵ S. Heppelmann,³² A. Hirsch,³⁴ G. W. Hoffmann,⁴³ S. Horvat,⁵⁵
 X. Huang,⁴⁵ H. Z. Huang,⁶ T. Huang,²⁸ B. Huang,⁸ T. J. Humanic,²⁹ P. Huo,⁴⁰ G. Igo,⁶ W. W. Jacobs,¹⁴
 A. Jentsch,⁴³ J. Jia,^{3, 40} K. Jiang,³⁷ S. Jowzaee,⁵³ E. G. Judd,⁴ S. Kabana,¹⁸ D. Kalinkin,¹⁴ K. Kang,⁴⁵
 D. Kapukchyan,⁴⁸ K. Kauder,⁵³ H. W. Ke,³ D. Keane,¹⁸ A. Kechechyan,¹⁷ Z. Khan,⁸ D. P. Kikoła,⁵² C. Kim,⁴⁸
 I. Kisiel,¹² A. Kisiel,⁵² L. Kochenda,²⁶ M. Kocmanek,¹¹ T. Kollegger,¹² L. K. Kosarzewski,⁵² A. F. Kraishan,⁴¹
 L. Krauth,⁴⁸ P. Kravtsov,²⁶ K. Krueger,² N. Kulathunga,⁴⁴ L. Kumar,³¹ J. Kvapil,¹⁰ J. H. Kwasizur,¹⁴ R. Lacey,⁴⁰
 J. M. Landgraf,³ K. D. Landry,⁶ J. Lauret,³ A. Lebedev,³ R. Lednický,¹⁷ J. H. Lee,³ C. Li,³⁷ W. Li,³⁹
 Y. Li,⁴⁵ X. Li,³⁷ J. Lidrych,¹⁰ T. Lin,¹⁴ M. A. Lisa,²⁹ P. Liu,⁴⁰ F. Liu,⁷ H. Liu,¹⁴ Y. Liu,⁴² T. Ljubicic,³
 W. J. Llope,⁵³ M. Lomnitz,²² R. S. Longacre,³ X. Luo,⁷ S. Luo,⁸ G. L. Ma,³⁹ L. Ma,³⁹ Y. G. Ma,³⁹ R. Ma,³
 N. Magdy,⁴⁰ R. Majka,⁵⁵ D. Mallick,²⁷ S. Margetis,¹⁸ C. Markert,⁴³ H. S. Matis,²² K. Meehan,⁵ J. C. Mei,³⁸
 Z. W. Miller,⁸ N. G. Minaev,³³ S. Mioduszewski,⁴² D. Mishra,²⁷ S. Mizuno,²² B. Mohanty,²⁷ M. M. Mondal,¹³
 D. A. Morozov,³³ M. K. Mustafa,²² Md. Nasim,⁶ T. K. Nayak,⁵¹ J. M. Nelson,⁴ M. Nie,³⁹ G. Nigmatkulov,²⁶
 T. Niida,⁵³ L. V. Nogach,³³ T. Nonaka,⁴⁶ S. B. Nurushev,³³ G. Odyniec,²² A. Ogawa,³ K. Oh,³⁵ V. A. Okorokov,²⁶
 D. Olvitt Jr.,⁴¹ B. S. Page,³ R. Pak,³ Y. Pandit,⁸ Y. Panebratsev,¹⁷ B. Pawlik,³⁰ H. Pei,⁷ C. Perkins,⁴ P. Pile,³
 J. Pluta,⁵² K. Poniatowska,⁵² J. Porter,²² M. Posik,⁴¹ N. K. Pruthi,³¹ M. Przybycien,¹ J. Putschke,⁵³ H. Qiu,³⁴
 A. Quintero,⁴¹ S. Ramachandran,¹⁹ R. L. Ray,⁴³ R. Reed,²³ M. J. Rehbein,⁹ H. G. Ritter,²² J. B. Roberts,³⁶
 O. V. Rogachevskiy,¹⁷ J. L. Romero,⁵ J. D. Roth,⁹ L. Ruan,³ J. Rusnak,¹¹ O. Rusnakova,¹⁰ N. R. Sahoo,⁴²
 P. K. Sahu,¹³ S. Salur,²² J. Sandweiss,⁵⁵ M. Saur,¹¹ J. Schambach,⁴³ A. M. Schmah,²² W. B. Schmidke,³
 N. Schmitz,²⁴ B. R. Schweid,⁴⁰ J. Seger,⁹ M. Sergeeva,⁶ R. Seto,⁴⁸ P. Seyboth,²⁴ N. Shah,³⁹ E. Shahaliev,¹⁷
 P. V. Shanmuganathan,²³ M. Shao,³⁷ M. K. Sharma,¹⁶ A. Sharma,¹⁶ W. Q. Shen,³⁹ Z. Shi,²² S. S. Shi,⁷
 Q. Y. Shou,³⁹ E. P. Sichtermann,²² R. Sikora,¹ M. Simko,¹¹ S. Singha,¹⁸ M. J. Skoby,¹⁴ D. Smirnov,³ N. Smirnov,⁵⁵
 W. Solyst,¹⁴ L. Song,⁴⁴ P. Sorensen,³ H. M. Spinka,² B. Srivastava,³⁴ T. D. S. Stanislaus,⁵⁰ M. Strikhanov,²⁶
 B. Stringfellow,³⁴ T. Sugiura,⁴⁶ M. Sumbera,¹¹ B. Summa,³² X. M. Sun,⁷ Y. Sun,³⁷ X. Sun,⁷ B. Surrow,⁴¹
 D. N. Svirida,¹⁵ A. H. Tang,³ Z. Tang,³⁷ A. Taranenko,²⁶ T. Tarnowsky,²⁵ A. Tawfik,⁵⁴ J. Thäder,²²
 J. H. Thomas,²² A. R. Timmins,⁴⁴ D. Tlusty,³⁶ T. Todoroki,³ M. Tokarev,¹⁷ S. Trentalange,⁶ R. E. Tribble,⁴²
 P. Tribedy,³ S. K. Tripathy,¹³ B. A. Trzeciak,¹⁰ O. D. Tsai,⁶ T. Ullrich,³ D. G. Underwood,² I. Upsal,²⁹
 G. Van Buren,³ G. van Nieuwenhuizen,³ A. N. Vasiliev,³³ F. Videbæk,³ S. Vokal,¹⁷ S. A. Voloshin,⁵³ A. Vossen,¹⁴
 F. Wang,³⁴ Y. Wang,⁷ G. Wang,⁶ Y. Wang,⁴⁵ J. C. Webb,³ G. Webb,³ L. Wen,⁶ G. D. Westfall,²⁵ H. Wieman,²²
 S. W. Wissink,¹⁴ R. Witt,⁴⁹ Y. Wu,¹⁸ Z. G. Xiao,⁴⁵ G. Xie,³⁷ W. Xie,³⁴ Z. Xu,³ N. Xu,²² Y. F. Xu,³⁹ Q. H. Xu,³⁸
 J. Xu,⁷ Q. Yang,³⁷ C. Yang,³⁸ S. Yang,³ Y. Yang,²⁸ Z. Ye,⁸ Z. Ye,⁸ L. Yi,⁵⁵ K. Yip,³ I. -K. Yoo,³⁵ N. Yu,⁷
 H. Zbroszczyk,⁵² W. Zha,³⁷ X. P. Zhang,⁴⁵ S. Zhang,³⁹ J. B. Zhang,⁷ J. Zhang,²² Z. Zhang,³⁹ S. Zhang,³⁷
 J. Zhang,²¹ Y. Zhang,³⁷ J. Zhao,³⁴ C. Zhong,³⁹ L. Zhou,³⁷ C. Zhou,³⁹ Z. Zhu,³⁸ X. Zhu,⁴⁵ and M. Zyzak¹²

(STAR Collaboration)

¹AGH University of Science and Technology, FPACS, Cracow 30-059, Poland

²Argonne National Laboratory, Argonne, Illinois 60439

³Brookhaven National Laboratory, Upton, New York 11973

⁴University of California, Berkeley, California 94720

- ⁵University of California, Davis, California 95616
⁶University of California, Los Angeles, California 90095
⁷Central China Normal University, Wuhan, Hubei 430079
⁸University of Illinois at Chicago, Chicago, Illinois 60607
⁹Creighton University, Omaha, Nebraska 68178
¹⁰Czech Technical University in Prague, FNSPE, Prague, 115 19, Czech Republic
¹¹Nuclear Physics Institute AS CR, 250 68 Prague, Czech Republic
¹²Frankfurt Institute for Advanced Studies FIAS, Frankfurt 60438, Germany
¹³Institute of Physics, Bhubaneswar 751005, India
¹⁴Indiana University, Bloomington, Indiana 47408
¹⁵Alikhanov Institute for Theoretical and Experimental Physics, Moscow 117218, Russia
¹⁶University of Jammu, Jammu 180001, India
¹⁷Joint Institute for Nuclear Research, Dubna, 141 980, Russia
¹⁸Kent State University, Kent, Ohio 44242
¹⁹University of Kentucky, Lexington, Kentucky 40506-0055
²⁰Lamar University, Physics Department, Beaumont, Texas 77710
²¹Institute of Modern Physics, Chinese Academy of Sciences, Lanzhou, Gansu 730000
²²Lawrence Berkeley National Laboratory, Berkeley, California 94720
²³Lehigh University, Bethlehem, Pennsylvania 18015
²⁴Max-Planck-Institut fur Physik, Munich 80805, Germany
²⁵Michigan State University, East Lansing, Michigan 48824
²⁶National Research Nuclear University MEPhI, Moscow 115409, Russia
²⁷National Institute of Science Education and Research, Bhubaneswar 751005, India
²⁸National Cheng Kung University, Tainan 70101
²⁹Ohio State University, Columbus, Ohio 43210
³⁰Institute of Nuclear Physics PAN, Cracow 31-342, Poland
³¹Panjab University, Chandigarh 160014, India
³²Pennsylvania State University, University Park, Pennsylvania 16802
³³Institute of High Energy Physics, Protvino 142281, Russia
³⁴Purdue University, West Lafayette, Indiana 47907
³⁵Pusan National University, Pusan 46241, Korea
³⁶Rice University, Houston, Texas 77251
³⁷University of Science and Technology of China, Hefei, Anhui 230026
³⁸Shandong University, Jinan, Shandong 250100
³⁹Shanghai Institute of Applied Physics, Chinese Academy of Sciences, Shanghai 201800
⁴⁰State University of New York, Stony Brook, New York 11794
⁴¹Temple University, Philadelphia, Pennsylvania 19122
⁴²Texas A&M University, College Station, Texas 77843
⁴³University of Texas, Austin, Texas 78712
⁴⁴University of Houston, Houston, Texas 77204
⁴⁵Tsinghua University, Beijing 100084
⁴⁶University of Tsukuba, Tsukuba, Ibaraki, Japan,305-8571
⁴⁷Southern Connecticut State University, New Haven, Connecticut 06515
⁴⁸University of California, Riverside, California 92521
⁴⁹United States Naval Academy, Annapolis, Maryland 21402
⁵⁰Valparaiso University, Valparaiso, Indiana 46383
⁵¹Variable Energy Cyclotron Centre, Kolkata 700064, India
⁵²Warsaw University of Technology, Warsaw 00-661, Poland
⁵³Wayne State University, Detroit, Michigan 48201
⁵⁴World Laboratory for Cosmology and Particle Physics (WLAPP), Cairo 11571, Egypt
⁵⁵Yale University, New Haven, Connecticut 06520

Fluctuations of conserved quantities such as baryon number, charge, and strangeness are sensitive to the correlation length of the hot and dense matter created in relativistic heavy-ion collisions and can be used to search for the QCD critical point. We report the first measurements of the moments of net-kaon multiplicity distributions in Au+Au collisions at $\sqrt{s_{\text{NN}}} = 7.7, 11.5, 14.5, 19.6, 27, 39, 62.4$, and 200 GeV. The collision centrality and energy dependence of the mean (M), variance (σ^2), skewness (S), and kurtosis (κ) for net-kaon multiplicity distributions as well as the ratio σ^2/M and the products $S\sigma$ and $\kappa\sigma^2$ are presented. Comparisons are made with Poisson and negative binomial baseline calculations as well as with UrQMD, a transport model (UrQMD) that does not include effects from the QCD critical point. Within current uncertainties, the net-kaon cumulant ratios appear to be monotonic as a function of collision energy.

I. INTRODUCTION

One primary goal of high energy heavy-ion collisions is to explore the phase structure of strongly interacting hot, dense nuclear matter. It can be displayed in the quantum chromodynamics (QCD) phase diagram, which is characterized by the temperature (T) and the baryon chemical potential (μ_B). Lattice QCD calculations suggest that the phase transition between the hadronic phase and the quark-gluon plasma (QGP) phase at large μ_B and low T is of the first order [1, 2], while in the low μ_B and high T region, the phase transition is a smooth crossover [3]. The end point of the first order phase boundary towards the crossover region is the so-called critical point [4, 5]. Experimental search for the critical point is one of the central goals of the beam energy scan (BES) program at the Relativistic Heavy-Ion Collider (RHIC) facility at Brookhaven National Laboratory.

Fluctuations of conserved quantities, such as baryon number (B), charge (Q), and strangeness (S) are sensitive to the QCD phase transition and QCD critical point [6–8]. Experimentally, one can measure the moments (mean (M), variance (σ^2), skewness (S), and kurtosis (κ)) of the event-by-event net-particle distributions (particle multiplicity minus antiparticle multiplicity), such as net-proton, net-kaon and net-charge multiplicity distributions in heavy-ion collisions. These moments are connected to the thermodynamic susceptibilities that can be computed in lattice QCD [5, 9–15] and in the hadron resonance gas model (HRG) [16–19]. They are expected to be sensitive to the correlation length (ξ) of the hot and dense medium created in the heavy-ion collisions [6]. Non-monotonic variation of fluctuations in conserved quantities with the colliding beam energy is considered to be one of the characteristic signature of the QCD critical point.

The moments σ^2 , S , and κ have been shown to be related to powers of the correlation length as ξ^2 , $\xi^{4.5}$ and ξ^7 [6], respectively. The n^{th} order susceptibilities $\chi^{(n)}$ are related to cumulant as $\chi^{(n)} = C_n/VT^3$ [8], where V, T are the volume and temperature of the system, C_n is the n^{th} order cumulant of multiplicity distributions. The moment products $S\sigma$ and $\kappa\sigma^2$ and the ratio σ^2/M are constructed to cancel the volume term. The moment products are related to the ratios of various orders of susceptibilities according to $\kappa\sigma^2 = \chi_i^{(4)}/\chi_i^{(2)}$ and $S\sigma = \chi_i^{(3)}/\chi_i^{(2)}$, where i indicates the conserved quantity. Due to the sensitivity to the correlation length and the connection with the susceptibilities, one can use the moments of conserved-quantity distributions to aid in the search for the QCD critical point and the QCD phase transition [6–8, 16, 20–30]. In addition, the moments of net-particle fluctuations can be used to determine freeze-out points on the QCD phase diagram by comparing directly to first-principle lattice QCD calculations [12]. Specifically, by comparing the lattice QCD results to the measured σ^2/M for net kaons, one can infer the hadronization temperature of strange quarks [31].

As a part of the BES, Au+Au collisions were run by RHIC with energies ranging from $\sqrt{s_{\text{NN}}} = 200$ GeV down to 7.7 GeV [32–34] corresponding to μ_B from 20 to 420 MeV. In this paper, we report the first measurements for the moments of net-kaon multiplicity distributions in Au+Au collisions at $\sqrt{s_{\text{NN}}} = 7.7, 11.5, 14.5, 19.6, 27, 39, 62.4$, and 200 GeV. These results are compared with baseline calculations (Poisson and negative binomial) and the Ultrarelativistic Quantum Molecular Dynamics (UrQMD, version 2.3) model calculations [35].

The manuscript is organized as follows. In section II, we define the observables used in the analysis. In section III, we describe the STAR (Solenoidal Tracker At RHIC) experiment at BNL and the analysis techniques. In section IV, we present the experimental results for the moments of the net-kaon multiplicity distributions in Au+Au collisions at RHIC BES energies. A summary is given in section V.

II. OBSERVABLES

Distributions can be characterized by the moments M , σ^2 , S , and κ as well as in terms of cumulants C_1, C_2, C_3 , and C_4 [36].

In the present analysis, we use N to represent particle multiplicity in one event and ΔN_K ($N_{K^+} - N_{K^-}$) the net-kaon number. The average value over the entire event ensemble is denoted by $\langle N \rangle$. Then the deviation of N from its mean value can be written as $\delta N = N - \langle N \rangle$. The various order cumulants of event-by-event distributions of N are defined as:

$$C_1 = \langle N \rangle \quad (1)$$

$$C_2 = \langle (\delta N)^2 \rangle \quad (2)$$

$$C_3 = \langle (\delta N)^3 \rangle \quad (3)$$

$$C_4 = \langle (\delta N)^4 \rangle - 3\langle (\delta N)^2 \rangle^2 \quad (4)$$

The moments can be written in terms of the cumulants as:

$$M = C_1, \sigma^2 = C_2, S = \frac{C_3}{(C_2)^{\frac{3}{2}}}, \kappa = \frac{C_4}{(C_2)^2} \quad (5)$$

In addition, the products of moments $\kappa\sigma^2$ and $S\sigma$ can be expressed in terms of cumulant ratios:

$$\kappa\sigma^2 = \frac{C_4}{C_2}, S\sigma = \frac{C_3}{C_2} \quad (6)$$

III. DATA ANALYSIS

The results presented in this paper are based on the data taken at STAR [37] for Au+Au collisions at $\sqrt{s_{\text{NN}}}$

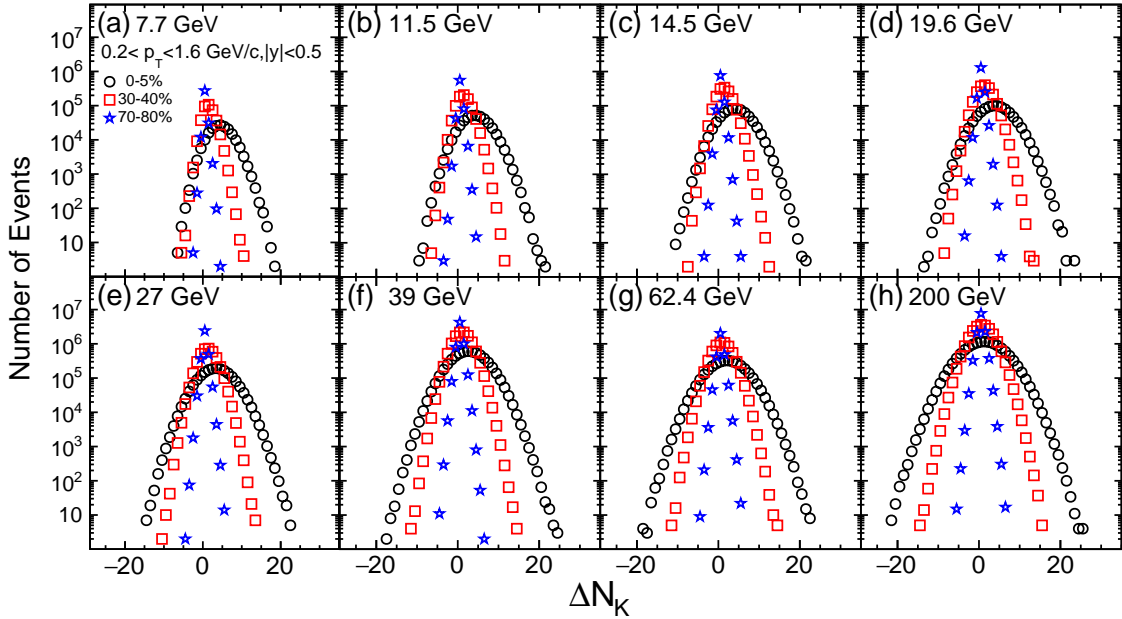


FIG. 1. (Color Online). Raw ΔN_K distributions in Au+Au collisions from $\sqrt{s_{\text{NN}}} = 7.7$ to 200 GeV for 0-5%, 30-40%, and 70-80% collision centralities at midrapidity. The distributions are not corrected for the finite centrality bin width effect nor the reconstruction efficiency.

= 7.7, 11.5, 14.5, 19.6, 27, 39, 62.4 and 200 GeV. The 7.7, 11.5, 39, 62.4, and 200 GeV data were collected in the year 2010, the 19.6 and 27 GeV data were collected in the year 2011, and the 14.5 GeV data were collected in the year 2014.

The STAR detector has a large uniform acceptance at midrapidity ($|\eta| < 1$) with excellent particle identification capabilities , i.e., allowing to identify kaons from other charged particles for $0.2 < p_T < 1.6 \text{ GeV}/c$. Energy loss (dE/dx) in the time projection chamber (TPC) [38] and mass-squared (m^2) from the time-of-flight detector (TOF) [39] are used to identify K^+ and K^- . To utilize the energy loss measured in the TPC, a quantity $n\sigma_X$ is defined as:

$$n\sigma_X = \frac{\ln[(dE/dx)_{\text{measured}}/(dE/dx)_{\text{theory}}]}{\sigma_X} \quad (7)$$

where $(dE/dx)_{\text{measured}}$ is the ionization energy loss from TPC, and $(dE/dx)_{\text{theory}}$ is the Bethe-Bloch [40] expectation for the given particle type (e.g. π, K, p). σ_X is the dE/dx resolution of TPC. We select K^+ and K^- particles by using a cut $|n\sigma_{K\alpha n}| < 2$ within transverse momentum range $0.2 < p_T < 1.6 \text{ GeV}/c$ and rapidity $|y| < 0.5$. The TOF detector measures the time of flight (t) of a particle from the primary vertex of the collision. Combined with the path length (L) measured in

the TPC, one can directly calculate the velocity (v) of the particles and their rest mass (m) using:

$$\beta = \frac{v}{c} = \frac{L}{ct} \quad (8)$$

$$m^2 c^2 = p^2 \left(\frac{1}{\beta^2} - 1 \right) = p^2 \left(\frac{c^2 t^2}{L^2} - 1 \right) \quad (9)$$

In this analysis, we use mass-squared cut $0.15 < m^2 < 0.4 \text{ GeV}^2/c^4$ to select K^+ and K^- within the p_T range $0.4 < p_T < 1.6 \text{ GeV}/c$ to get high purity of kaon sample (better than 99%). For the p_T range $0.2 < p_T < 0.4 \text{ GeV}/c$, we use only the TPC to identify K^+ and K^- .

The collision centrality is determined using the efficiency-uncorrected charged particle multiplicity excluding identified kaons within pseudorapidity $|\eta| < 1.0$ measured with the TPC. This definition maximizes the number of particles used to determine the collision centrality and avoids self-correlations between the kaons used to calculate the moments and kaons in the reference multiplicity [41]. Using the distribution of this reference multiplicity along with the Glauber model [42] simulations, the collision centrality is determined. This reference multiplicity is similar in concept to the reference multiplicity used by STAR to study moments of net-proton distributions [29], where the reference multiplicity was calculated using all charged particles within

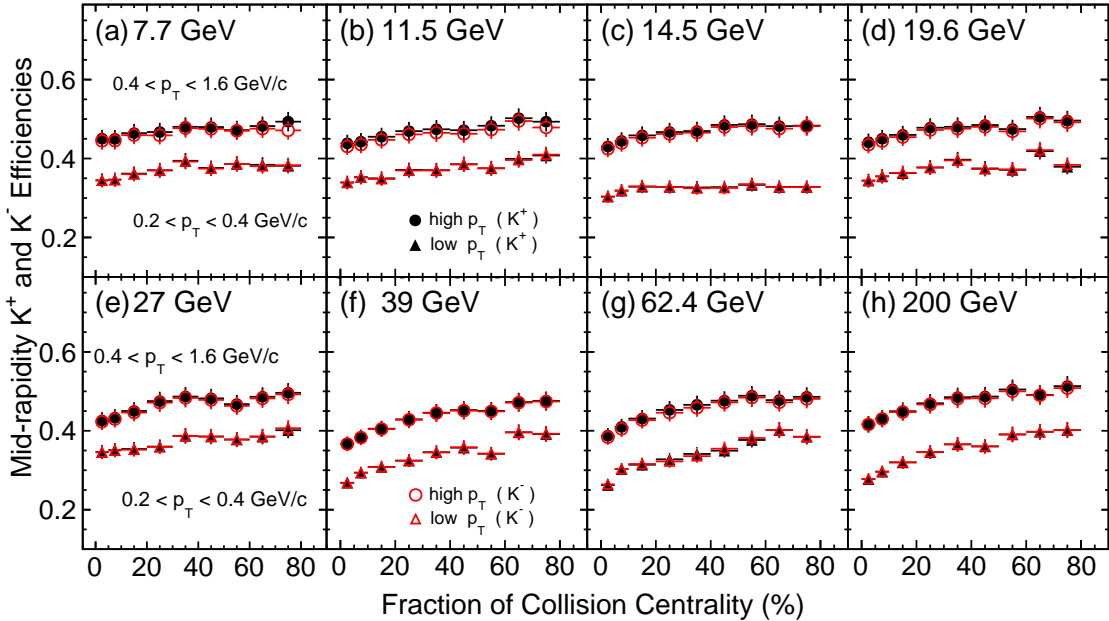


FIG. 2. (Color Online). Collision centrality dependence of the p_T -averaged efficiencies in Au+Au collisions. For the lower p_T range ($0.2 < p_T < 0.4 \text{ GeV}/c$), only the TPC is used. For the higher p_T range ($0.4 < p_T < 1.6 \text{ GeV}/c$), both the TPC and TOF are used for particle identification (PID).

$|\eta| < 1.0$ excluding identified protons and antiprotons. Using this definition, collision centrality bins of 0-5%, 5-10%, 10-20%, 20-30%, 30-40%, 40-50%, 50-60%, 60-70%, and 70-80% of the multiplicity distributions were used with 0-5% representing the most central collisions.

Figure 1 shows the raw event-by-event net-kaon multiplicity ($\Delta N_K = N_{K^+} - N_{K^-}$) distributions in Au+Au collisions at $\sqrt{s_{\text{NN}}} = 7.7$ to 200 GeV for three collision centralities, i.e. 0-5%, 30-40%, and 70-80%. For the 0-5% central collision, the peaks of the distributions are close to zero at high energies, and shift towards the positive direction as the energy decreases. This is because the pair production of K^+ and K^- dominates at high energies while the production of K^+ is dominated by the associated production via reaction channel $NN \rightarrow NAK^+$ at lower energy [43]. Those distributions are not corrected for the finite centrality bin width effect and also track reconstruction efficiency. However, all the cumulants and their ratios presented in this paper are corrected for the finite centrality bin width effect [41] and efficiency of K^+ and K^- .

The moments and cumulants can be expressed in terms of factorial moments, which can be easily corrected for efficiency [44, 45]. The efficiency correction is done by assuming the response function of the efficiency is a binomial probability distribution. Figure 2 shows the collision centrality dependence of the p_T -averaged efficiencies of tracking and PID combined for two p_T ranges. One can

see that at the lower p_T range ($0.2 < p_T < 0.4 \text{ GeV}/c$), kaons have a lower efficiency compared with the higher p_T range ($0.4 < p_T < 1.6 \text{ GeV}/c$). The efficiencies increase monotonically with the centrality changing from most central ($0 \sim 5\%$) to peripheral ($70 \sim 80\%$). K^+ and K^- have similar efficiencies.

By calculating the covariance between the various order factorial moments, one can obtain the statistical uncertainties for the efficiency corrected moments based on the error propagation derived from the Delta theorem [41, 45, 46]. The statistical uncertainties of various order cumulants and cumulant ratios strongly depend on the width (σ) of the measured multiplicity distributions as well as the efficiencies (ε). One can roughly estimate the statistical uncertainties of $S\sigma$ and $\kappa\sigma^2$ as $\text{error}(S\sigma) \propto \frac{\sigma}{\varepsilon^{3/2}}$ and $\text{error}(\kappa\sigma^2) \propto \frac{\sigma^2}{\varepsilon^2}$. That explains why we observe larger statistical uncertainties for central than peripheral collisions, as on the width of the net-kaon distributions grows from peripheral to central. Furthermore, due to the smaller detection efficiency of kaons than the protons, we observe larger statistical uncertainties of cumulants and cumulant ratios than those of the net-proton fluctuations [29]. Systematic uncertainties are estimated by varying the following track quality cuts: distance of closest approach, the number of fit points used in track reconstruction, the dE/dx selection criteria for identification, and additional 5% uncertainties in the reconstruction efficiency. The typical systematic

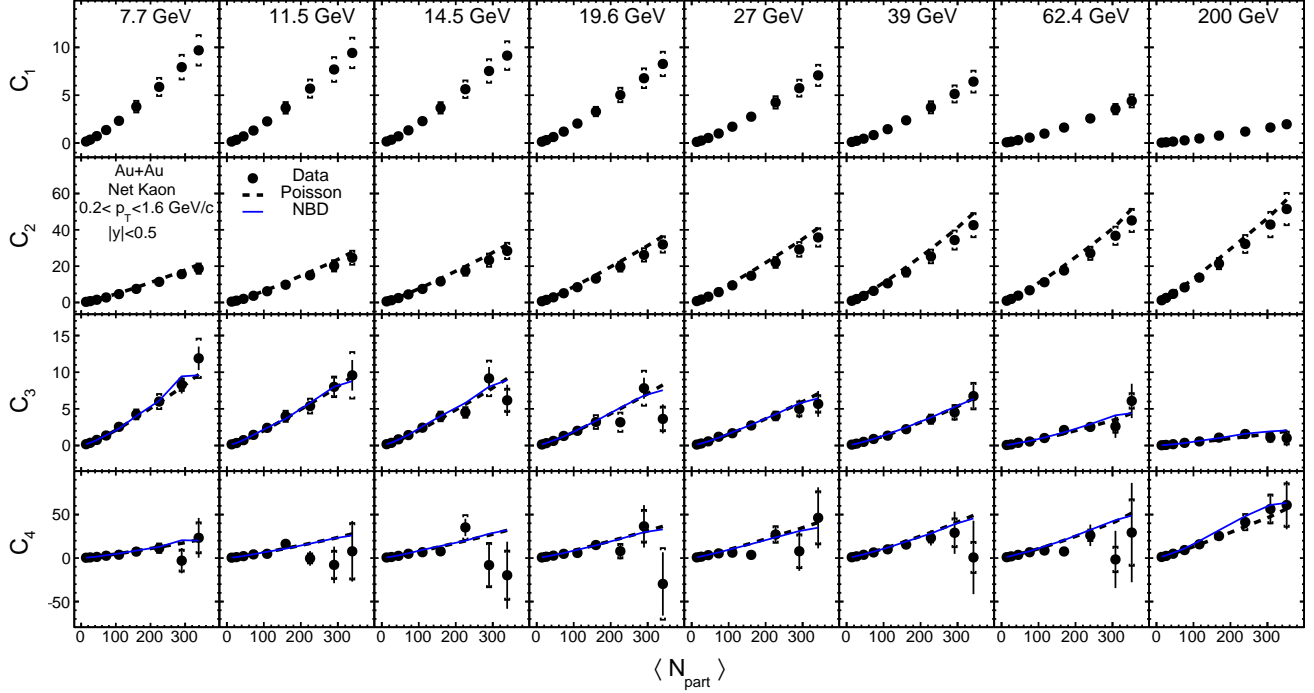


FIG. 3. (Color Online). Collision centrality dependence of cumulants (C_1 , C_2 , C_3 , and C_4) of ΔN_K distributions for Au+Au collisions at $\sqrt{s_{\text{NN}}} = 7.7 - 200$ GeV. The error bars are statistical uncertainties and the caps represent systematic uncertainties. The Poisson and NBD expectations are shown as dashed and blue solid lines, respectively.

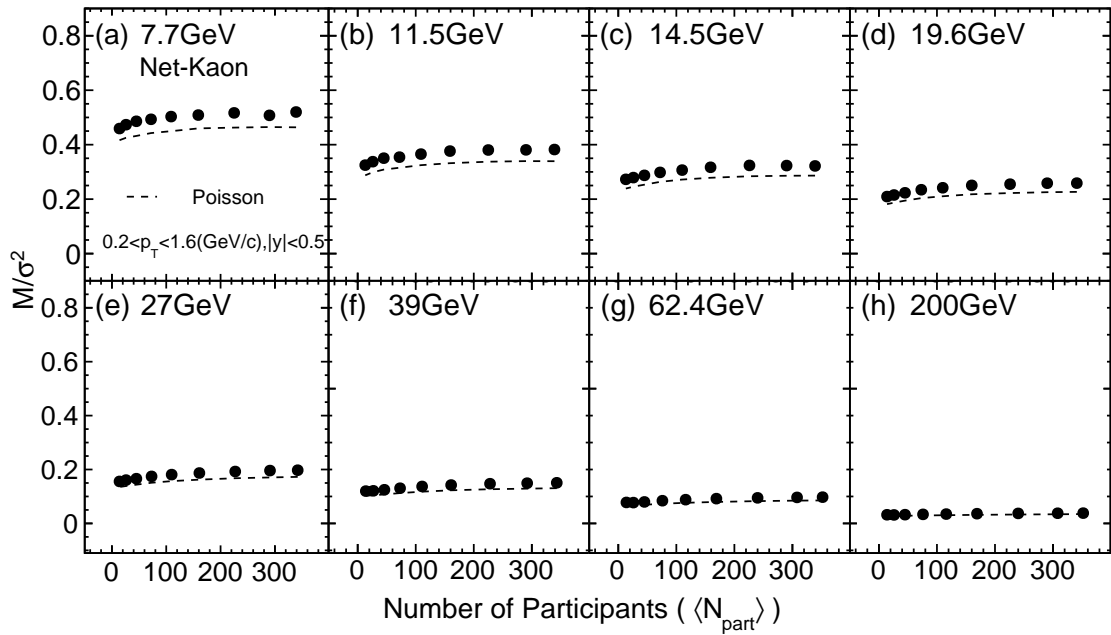


FIG. 4. (Color Online). Collision centrality dependence of M/σ^2 for ΔN_K distributions in Au+Au collisions at $\sqrt{s_{\text{NN}}} = 7.7 - 200$ GeV. The Poisson expectations are shown as dashed lines.

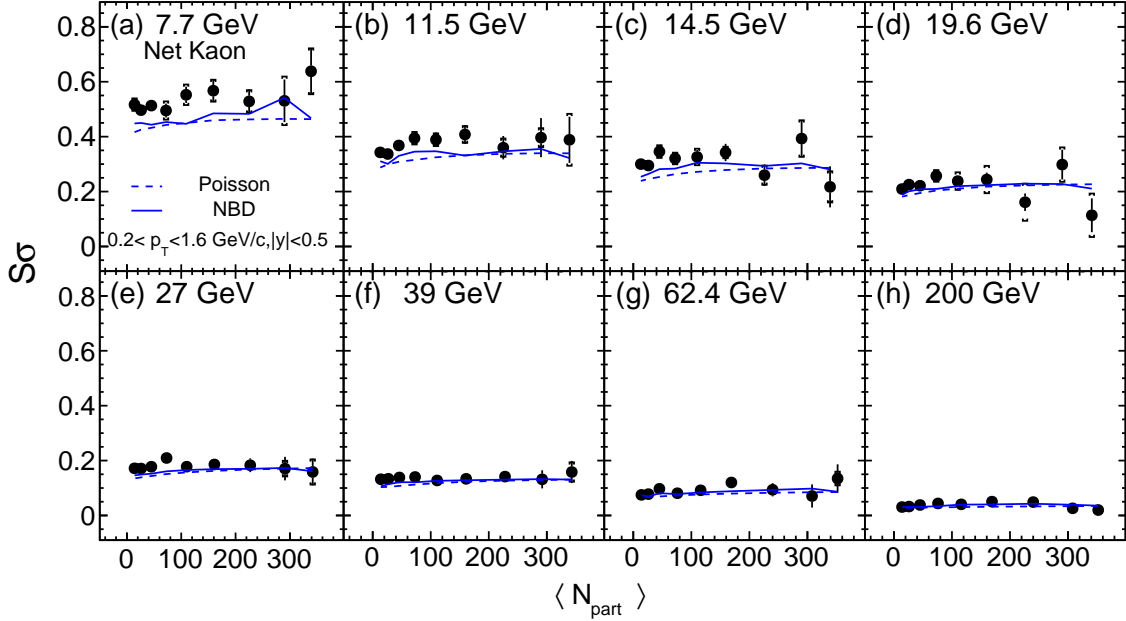


FIG. 5. (Color Online). Collision centrality dependence of the $S\sigma$ for ΔN_K distributions from Au+Au collisions at $\sqrt{s_{NN}} = 7.7 - 200$ GeV. The error bars are statistical uncertainties and the caps represent systematic uncertainties. The Poisson (dashed line) and NBD (blue solid line) expectations are also shown.

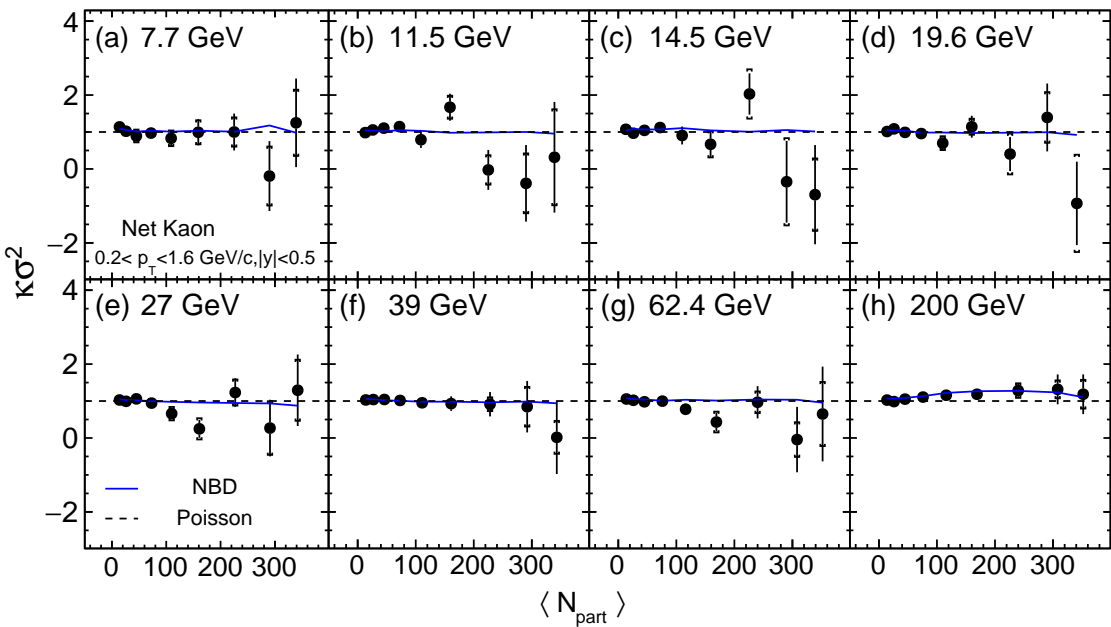


FIG. 6. (Color Online). Collision centrality dependence of the $\kappa\sigma^2$ for ΔN_K distributions from Au+Au collisions at $\sqrt{s_{NN}} = 7.7 - 200$ GeV. The error bars are statistical uncertainties and the caps represent systematic uncertainties. The Poisson (dashed-line) and NBD (blue-solid-line) expectations are also shown.

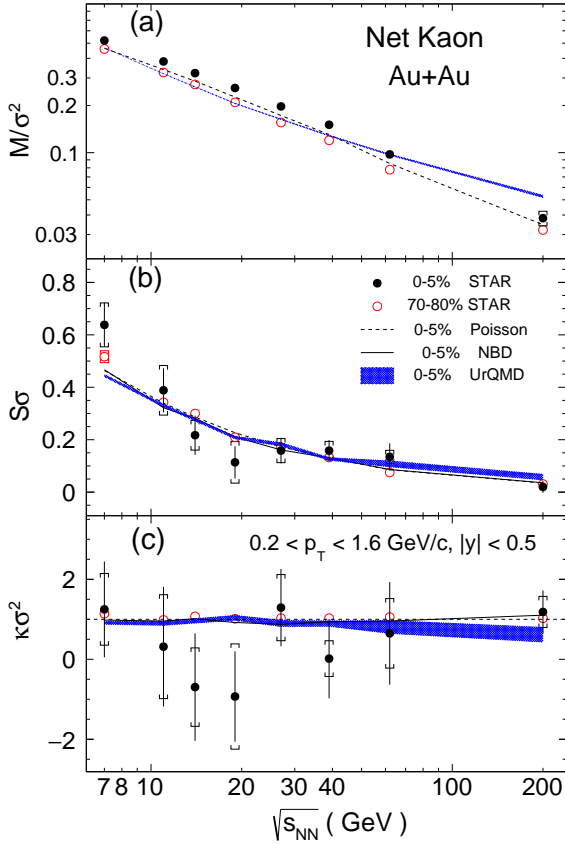


FIG. 7. (Color Online). Collision energy dependence of the values of M/σ^2 , $S\sigma$, $\kappa\sigma^2$ for ΔN_K multiplicity distributions from 0-5% most central and 70-80% peripheral collisions in Au+Au collisions at $\sqrt{s_{NN}} = 7.7, 11.5, 14.5, 19.6, 27, 39, 62.4$ and 200 GeV. The error bars are statistical uncertainties and the caps represent systematic uncertainties. The expectations from Poisson and NBD and the results of the UrQMD model calculations are all from the 0-5% centrality.

uncertainties are of the order of 15% for C_1 and C_2 , 21% for C_3 , and 65% for C_4 . The statistical and systematic (caps) errors are presented separately in the figures.

IV. RESULTS

Figure 3 shows the centrality dependence of cumulants ($C_1 - C_4$) of net-kaon (ΔN_K) multiplicity distributions in Au+Au collisions at $\sqrt{s_{NN}}=7.7-200$ GeV. The collisions centralities are represented by the average number of participating nucleons ($\langle N_{\text{part}} \rangle$), which are obtained by Glauber model simulation. The efficiency corrections have been done using the values shown in Fig. 2. In general, the various order cumulants show a nearly linear variation with $\langle N_{\text{part}} \rangle$, which can be understood as the additivity property of the cumulants by increasing the volume of the system. This reflects the fact that the

cumulants are extensive quantities that are proportional to the system volume. The decrease of the C_1 and C_3 values with increasing collision energy indicates that the ratio K^+/K^- approaches unity for the higher collision energies. Figure 3 also shows the Poisson and negative binomial distribution (NBD) [47, 48] expectations. The Poisson baseline is constructed using the measured mean values of the multiplicity distributions of K^+ and K^- , while the NBD baseline is constructed using both means and variances. Assuming that the event-by-event multiplicities of K^+ and K^- are independent random variables, the Poisson and NBD assumptions provide references for the moments of the net-kaon multiplicity distributions. Within uncertainties, the measured cumulants values of C_3 and C_4 are consistent with both the Poisson and NBD baselines for most centralities.

The ratios between different order cumulants are taken to cancel the volume dependence. Figures 4, 5, and 6 show the $\langle N_{\text{part}} \rangle$ dependence of ΔN_K distributions for cumulant ratios C_1/C_2 ($=M/\sigma^2$), C_3/C_2 ($=S\sigma$), and C_4/C_2 ($=\kappa\sigma^2$), respectively. The values of C_1/C_2 , shown in Fig. 4, systematically decrease with increasing collision energy for all centralities. The Poisson baseline for C_1/C_2 slightly underestimates the data, indicating possible correlations between K^+ and K^- production. For C_3/C_2 ($=S\sigma$) in Fig. 5, the Poisson and NBD expectations are observed to be lower than the measured $S\sigma$ values at low collision energies. The measured values for C_4/C_2 ($=\kappa\sigma^2$) in Fig. 6 are consistent with both the Poisson and NBD baselines within uncertainties.

The collision energy dependence of the cumulant ratios for ΔN_K distributions in Au+Au collisions are presented in Fig. 7. The results are shown in two collision centrality bins, one corresponding to most central (0-5%) and the other to peripheral (70-80%) collisions. Expectations from the Poisson and NBD baselines are derived for central (0-5%) collisions. The values of M/σ^2 decrease as the collision energy increases, and are larger for central collisions compared with the peripheral collisions. For most central collisions, the Poisson baseline for C_1/C_2 slightly underestimates the data. Within uncertainties, the values of $S\sigma$ and $\kappa\sigma^2$ are consistent with both the Poisson and NBD baselines in central collisions. The blue bands give the results from the UrQMD model calculations for central (0-5%) Au+Au collisions. The width of the bands represents the statistical uncertainties. The UrQMD calculations for $S\sigma$, and $\kappa\sigma^2$ are consistent with the measured values within uncertainties [49]. A QCD based model calculation suggests that, due to heavy mass of the strange-quark, the sensitivity of the net-kaon (ΔN_K) fluctuations is less than that of the net-proton (ΔN_p) [50]. A much high statistics dataset is needed for the search of the QCD critical point with strangeness.

V. SUMMARY

In heavy-ion collisions, fluctuations of conserved quantities, such as net-baryon, net-charge and net-strangeness numbers, are sensitive observables to search for the QCD critical point. Near the QCD critical point, those fluctuations are expected to have similar energy dependence behavior. Experimentally, the STAR experiment has published the energy dependence of the net-proton (proxy for net-baryon) [29] and net-charge [30] fluctuations in Au+Au collisions from the first phase of the beam energy scan at RHIC. In this paper, we present the first measurements of the moments of net-kaon (proxy for net-strangeness) multiplicity distributions in Au+Au collisions from $\sqrt{s_{\text{NN}}} = 7.7$ to 200 GeV. The measured M/σ^2 values decrease monotonically with increasing collision energy. The Poisson baseline for C_1/C_2 slightly underestimates the data. No significant collision centrality dependence is observed for both $S\sigma$ and $\kappa\sigma^2$ at all energies. For $C_3/C_2 (=S\sigma)$, the Poisson and NBD expectations are lower than the measured $S\sigma$ values at low collision energies. The measured values for $C_4/C_2 (=S\sigma^2)$ are consistent with both the Poisson and NBD baselines within uncertainties. UrQMD calculations for $S\sigma$ and $\kappa\sigma^2$ are consistent with data for the most central 0-5% Au+Au collisions. Within current uncertainties, the net-kaon cumulant ratios appear to be monotonic as a function of collision energy. The moments of net-kaon multiplicity distributions presented here can be used to extract

freeze-out conditions in heavy-ion collisions by comparing to Lattice QCD calculations. Future high precision measurements will be made for the net-kaon fluctuations in the second phase of the RHIC Beam Energy Scan during 2019-2020.

ACKNOWLEDGMENTS

We thank the RHIC Operations Group and RCF at BNL, the NERSC Center at LBNL, and the Open Science Grid consortium for providing resources and support. This work was supported in part by the Office of Nuclear Physics within the U.S. DOE Office of Science, the U.S. National Science Foundation, the Ministry of Education and Science of the Russian Federation, National Natural Science Foundation of China, Chinese Academy of Science, the Ministry of Science and Technology of China and the Chinese Ministry of Education, the National Research Foundation of Korea, GA and MSMT of the Czech Republic, Department of Atomic Energy and Department of Science and Technology of the Government of India; the National Science Centre of Poland, National Research Foundation, the Ministry of Science, Education and Sports of the Republic of Croatia, RosAtom of Russia and German Bundesministerium fur Bildung, Wissenschaft, Forschung und Technologie (BMBF) and the Helmholtz Association.

-
- [1] S. Ejiri, *Phys. Rev. D* **78**, 074507 (2008).
 - [2] M. Alford, K. Rajagopal, and F. Wilczek, *Phys. Lett. B* **422**, 247 (1998).
 - [3] Y. Aoki, G. Endrődi, Z. Fodor, S. D. Katz, and K. K. Szabó, *Nature* **443**, 675 (2006).
 - [4] M. Stephanov, *Int. J. Mod. Phys. A* **20**, 4387 (2005).
 - [5] R. V. Gavai, *Contemporary Physics* **57**, 350 (2016).
 - [6] M. A. Stephanov, *Phys. Rev. Lett.* **102**, 032301 (2009).
 - [7] M. A. Stephanov, *Phys. Rev. Lett.* **107**, 052301 (2011).
 - [8] S. Gupta, X. Luo, B. Mohanty, H. G. Ritter, and N. Xu, *Science* **332**, 1525 (2011).
 - [9] R. V. Gavai and S. Gupta, *Phys. Rev. D* **78**, 114503 (2008).
 - [10] M. Cheng *et al.*, *Phys. Rev. D* **79**, 074505 (2009).
 - [11] A. Bazavov *et al.*, *Phys. Rev. D* **86**, 034509 (2012).
 - [12] A. Bazavov *et al.*, *Phys. Rev. Lett.* **109**, 192302 (2012).
 - [13] S. Borsányi, Z. Fodor, S. D. Katz, S. Krieg, C. Ratti, and K. K. Szabó, *Phys. Rev. Lett.* **111**, 062005 (2013).
 - [14] P. Alba *et al.*, *Phys. Lett. B* **738**, 305 (2014).
 - [15] F. Karsch *et al.*, *Nucl. Phys. A* **956**, 352 (2016).
 - [16] F. Karsch and K. Redlich, *Phys. Lett. B* **695**, 136 (2011).
 - [17] P. Garg *et al.*, *Phys. Lett. B* **726**, 691 (2013).
 - [18] J. Fu, *Phys. Lett. B* **722**, 144 (2013).
 - [19] M. Nahrgang, M. Bluhm, P. Alba, R. Bellwied, and C. Ratti, *Eur. Phys. J. C* **75**, 573 (2015).
 - [20] B. Friman, *Nucl. Phys. A* **928**, 198 (2014).
 - [21] S. Mukherjee, R. Venugopalan, and Y. Yin, *Phys. Rev. C* **92**, 034912 (2015).
 - [22] M. Nahrgang, *Nucl. Phys. A* **956**, 83 (2016).
 - [23] J.-W. Chen, J. Deng, and L. Labun, *Phys. Rev. D* **92**, 054019 (2015).
 - [24] J.-W. Chen, J. Deng, H. Kohyama, and L. Labun, *Phys. Rev. D* **93**, 034037 (2016).
 - [25] V. Vovchenko, D. V. Anchishkin, M. I. Gorenstein, and R. V. Poberezhnyuk, *Phys. Rev. C* **92**, 054901 (2015).
 - [26] L. Jiang, P. Li, and H. Song, *Phys. Rev. C* **94**, 024918 (2016).
 - [27] M. Asakawa, S. Ejiri, and M. Kitazawa, *Phys. Rev. Lett.* **103**, 262301 (2009).
 - [28] B. J. Schaefer and M. Wagner, *Phys. Rev. D* **85**, 034027 (2012).
 - [29] L. Adamczyk (STAR Collaboration), *et al.*, *Phys. Rev. Lett.* **112**, 032302 (2014).
 - [30] L. Adamczyk (STAR Collaboration), *et al.*, *Phys. Rev. Lett.* **113**, 092301 (2014).
 - [31] J. Noronha-Hostler *et al.*, *Journal of Physics: Conference Series* **779**, 012050 (2017).
 - [32] M. M. Aggarwal, *et al.*, *arXiv:1007.2613*, (2010).
 - [33] B. I. Abelev *et al.* (STAR Collaboration), *Phys. Rev. C* **81**, 024911 (2010).
 - [34] STAR Internal Note - SN0493, 2009.
 - [35] M. Bleicher *et al.*, *J. Phys. G* **25**, 1859 (1999).
 - [36] A. Hald, *International Statistical Review* **68**, 137 (2000).

- [37] K. H. Ackermann, *et al.*, *Nucl. Ins. and Meth. A* **499**, 624 (2003).
- [38] M. Anderson, *et al.*, *Nucl. Ins. and Meth. A* **499**, 659 (2003).
- [39] W. J. Llope, *Nucl. Ins. and Meth. B* **241**, 306 (2005).
- [40] H. Bichsel, *Nucl. Ins. and Meth. A* **562**, 154 (2006).
- [41] X. Luo, J. Xu, B. Mohanty, and N. Xu, *J. Phys. G* **40**, 105104 (2013).
- [42] M. L. Miller, K. Reygers, S. J. Sanders, and P. Steinberg, *Annu. Rev. Nucl. Part. Sci.* **57**, 205 (2007).
- [43] C. Zhou, J. Xu, X. Luo, and F. Liu, *Phys. Rev. C* **96**, 014909 (2017).
- [44] A. Bzdak and V. Koch, *Phys. Rev. C* **91**, 027901 (2015).
- [45] X. Luo, *Phys. Rev. C* **91**, 034907 (2015).
- [46] X. Luo, *J. Phys. G* **39**, 025008 (2012), arXiv:1109.0593 [physics.data-an].
- [47] X. Luo, B. Mohanty, and N. Xu, *Nucl. Phys. A* **931**, 808 (2014).
- [48] T. J. Tarnowsky and G. D. Westfall, *Physics Letters B* **724**, 51 (2013).
- [49] J. Xu, S. Yu, F. Liu, and X. Luo, *Phys. Rev. C* **94**, 024901 (2016).
- [50] W. Fan, X. Luo, and H.-S. Zong, *Int. J. Mod. Phys. A* **32**, 1750061 (2017).